JOURNAL OF GEOPHYSICAL RESEARCH, VOL. 101, NO. D5, PAGES 9315–9321, APRIL 27, 1996

Comparison of air mass computations

James Slusser,[1] Kyle Hammond,[2] Arve Kylling, and Knut Stamnes
Geophysical Institute, University of Alaska, Fairbanks

Lori Perliski
Geophysical Fluids Dynamics Laboratory, Princeton, New Jersey

Arne Dahlback
Norwegian Institute for Air Research, Kjeller, Norway

Donald Anderson and Robert DeMajistre
Johns Hopkins University, Applied Physics Laboratory, Laurel, Maryland

Abstract. Knowledge of air mass is vital for the interpretation of twilight measurements of trace gases, as well as the conversion of measured slant column amounts to vertical abundances for comparison with model predictions. Radiative transfer computations were used to determine NO_2 air mass values for clear skies at 450 and 650 nm using a discrete ordinate (two different formulations), Monte Carlo, and an integral equation method. All four methods yielded agreement to within 6% at a solar zenith angle of 90° when the absorber was located in the stratosphere. For a tropospheric absorber, differences as large as 21% occurred at 90°. Since only the Monte Carlo method treats the scattered radiation in spherical geometry, it is more accurate for computing tropospheric air masses where multiple scattering is significant. The other three models use a conceptual approximation by treating the scattered radiation in plane parallel geometry. However, for absorbers in the stratosphere, major saving of computing time without any loss of accuracy is obtained using the discrete ordinate or integral equation method as compared to the Monte Carlo method.

1. Introduction

Spectroscopic measurements of scattered light to determine the slant column abundance of trace gases such as NO_2, OClO, and BrO make use of long optical paths through the atmosphere to maximize absorption. The air mass is the ratio of the slant column to vertical column abundance. Accurate determination of the air mass requires access to a good radiative transfer model and knowledge of the profile of the absorbing gas. Twilight observations of the zenith-sky radiance are commonly used to enhance the optical path through the atmosphere. Thus *Brewer* [1973], *Noxon* [1975], *Harrison* [1979], *McKenzie and Johnston* [1982], *Mount et al.* [1987] and *Pommereau and Goutail* [1988] used visible light spectrometers pointed at the zenith sky to measure the differential absorption of NO_2 during twilight. *Solomon et al.* [1989] and *Schiller et al.* [1990] extended the technique to measure OClO and BrO. Unlike the direct solar beam, which in the absence of refraction travels along a straight optical path, scattered or diffuse skylight travels along a random-walk path before reaching the detector.

Air mass values are used to convert measured slant column abundances to their vertical counterparts for comparison with column abundances predicted by photochemical models. They are also required to retrieve the vertical profile of the absorber from a time series of slant column abundances derived from scattered light measurements [*McKenzie et al.*, 1991]. Air mass values for a given solar zenith angle depend on the abundance of scattering particles in the atmosphere and therefore on the aerosol loading and its spatial distribution. In the presence of significant aerosol loading, it is crucial to know whether changes in the measured slant column abundances are due to real changes in absorber amounts, changes in air mass values due to the aerosols, or both [*Johnston et al.*, 1992; *Perliski and Solomon*, 1992]. Accurate computations of air mass values for a variety of atmospheric conditions are therefore essential in order to make reliable retrievals of stratospheric trace gases from remotely sensed radiation measurements.

Computation of air mass requires a rather complete knowledge of the optical properties of the atmosphere, including cross sections for absorption and scattering as well as profiles of radiatively active atmospheric constituents from which the optical depth, single-scattering albedo, and phase function may be determined. Spherical geometry must be considered for the large solar zenith angles used, as must the effects of multiple scattering for tropospheric trace species. The effects of surface albedo were shown to be insignificant in the case of stratospheric absorbers [*Perliski and Solomon*, 1993] and will be neglected in the computations that follow. The reason is that light reaching the stratosphere, after being reflected by the

[1]Now at Centre for Atmospheric Science, Department of Chemistry, Cambridge University, Cambridge, England.
[2]Now at Department of Physics, University of Minnesota, Minneapolis.

Paper number 96JD00054.
0148-0227/96/96JD-00054$05.00

lower atmosphere and surface, is unlikely to be scattered back to the detector due to the small-scattering optical depth of the stratosphere. The effect of refraction will be omitted, although refraction becomes increasingly important as the solar zenith angle gets larger [*Perliski and Solomon*, 1993].

Different methods have been utilized to compute air mass [*Sarkissian et al.*, 1995]. The aim of this paper is to compare the methods and results of four different ways to compute air mass. Computations for clear-sky and isotropic scattering made with the discrete ordinate (using two formulations), Monte Carlo, and integral equation methods are presented and compared. The sources and the significance of the differences between the results obtained by these methods are discussed.

After describing how air mass is calculated in section 2, we describe the different radiative transfer models in section 3. The results are presented in section 4 and our conclusions are provided in section 5.

2. Theory

Radiative Transfer

The incremental vertical optical depth, $d\tau_j$, of an infinitesimal layer of thickness, dz (cm), containing an absorbing and scattering species, j, is given by

$$d\tau_j = \sigma_j n_j(z)\, dz = (\sigma_j^{abs} + \sigma_j^{sca}) n_j(z)\, dz \tag{1}$$

where σ_j (cm^2) is the sum of the absorption (σ_j^{abs}) and scattering (σ_j^{sca}) cross sections, $n_j(z)$ (cm^{-3}) is the concentration of the absorbing/scattering species as a function of height. The vertical optical depth of a layer of finite thickness, Δz, is

$$\tau_j = \sigma_j \int_{\Delta z} n_j(z)\, dz = \sigma_j \Delta N_j \tag{2}$$

where ΔN_j is the vertical column abundance of the layer. For simplicity of exposition we have omitted the temperature dependence of the cross section. The total optical depth is obtained by summing over species

$$\tau = \sum_j \tau_j = \sum_j \sigma_j \Delta N_j. \tag{3}$$

In general, a beam of light incident on the layer makes an angle θ with respect to the normal. Compared to vertical incidence, this results in a longer pathlength, dz', and a larger slant optical depth, $\tau_s = \tau \sec \theta$, for a plane-parallel slab. The equation of radiative transfer is

$$\frac{dI(\tau, \hat{\Omega})}{d\tau} = -I(\tau, \hat{\Omega}) + S(\tau, \hat{\Omega}) \tag{4a}$$

where we have dropped the subscript s from the τ_s for convenience. Here I and S are the intensity and source function, respectively, at position τ_s in direction $\hat{\Omega}$. In the visible part of the spectrum the source function S is dominated by scattering. Equation (4a) must be solved subject to appropriate boundary conditions which in our case consist of specifying the incoming solar flux normal to the beam, F^s, the cosine of the solar zenith angle, μ_0, and the surface albedo. Alternatively, we may consider the integral equation satisfied by the source function. For isotropic scattering it may be written as

$$S(\tau) = \frac{a(\tau) F^s}{4\pi} e^{-\tau/\mu_0} + \frac{a(\tau)}{2} \int_0^{\tau^*} d\tau' E_1(|\tau - \tau'|) S(\tau') \tag{4b}$$

where $a(\tau)$ is the single-scattering albedo and E_1 is the exponential integral [$E_n(u) = \int_1^\infty dx(e^{-ux}/x^n)$]. The first term is due to single scattering, while the second term is the contribution to the source function from multiply scattered photons.

Assuming that we know (or have solved for) the source function S, we may obtain the intensity by integrating along the line of sight from a point P_1 to another point P_2. The result is

$$I[\tau(P_2), \hat{\Omega}] = I[\tau(P_1), \hat{\Omega}] e^{-\tau(P_1,P_2)} + \int_{\tau(P_1)}^{\tau(P_2)} dt S(t, \hat{\Omega}) e^{-t(P,P_2)}. \tag{5}$$

This equation states that the intensity at point P_2 (the detector in our case) coming from the atmosphere in the beam direction P_1P_2 (the zenith direction in our case) consists of two parts: (1) the contribution from the intensity incident at point P_1, which has been attenuated by the factor $e^{-\tau(P_1,P_2)}$, the beam transmittance, and (2) the contribution from emission (due to scattering) from those parts of the atmosphere that lie along the beam. Note that each differential contribution $S(t, \hat{\Omega})\, dt$ is weighted by the appropriate transmittance $e^{-t(P, P_2)}$, where P denotes an arbitrary point along the straight line (ignoring refraction) between P_1 and P_2.

In the absence of internal sources ($S = 0$) the integral term of (5) disappears so that it becomes just the Beer-Lambert law. Also, (4a) becomes simply

$$\frac{dI}{I} = -d\tau_s \quad \text{or} \quad \frac{d(\ln I)}{d\tau_s} = -1. \tag{6}$$

This equation describes the propagation of solar radiation through the atmosphere in the absence of scattering contributions to the beam intensity. If refraction is important, the intensity I should be replaced by I/n^2 where n is the index of refraction. We will assume that the index of refraction is constant, equal to unity, in this paper. Equation (6) leads to the following simple expression for the slant optical path

$$\tau_s = -\ln \frac{I}{I_0} \tag{7}$$

where I_0 is the incident intensity and I is the intensity after attenuation.

Scattered Light Transmission and Air Mass or Path Enhancement

For scattered light measurements the detector typically accepts light from a small solid angle around the direction of observation. We shall assume here that this direction is along the zenith. Diffuse atmospheric skylight is described by (5) rather than (6) because the intensity at the ground depends on the scattered contributions from each altitude and the multiple scattering and absorption of that light on its migratory path to the detector. The intensity of singly scattered light from a specific altitude in a given direction is proportional to the product of the direct solar radiation reaching that level (which increases with altitude), the scattering cross section including its angular dependence (phase function), the molecular density (which decreases with altitude), and the concentration of scattering particles. The zenith intensity at the ground is the sum of

singly and multiply scattered downwelling light from each level, attenuated on its way to the ground as described in (5). This intensity depends on the solar zenith angle as well as the vertical distribution of scatterers and absorbers.

To define air mass, it is useful to consider a model atmosphere with L layers, in which the layer denoted by l has an optical depth τ_l. By solving the radiative transfer equation (see (4) or (13) below), we may compute the zenith intensity at the ground, I. Suppose now that we increase the optical depth of layer l by $d\tau_{jl}^{abs}$ (due to the enhancement of a particular absorber denoted by j) and compute the resulting zenith intensity, I'. Although the light measured by the detector will not follow (6) but rather (5) (or (13) below), we may define the air mass or path enhancement factor δ_{jl} as

$$\delta_{jl} = \frac{d(\ln I)}{d\tau_{jl}^{abs}}. \tag{8}$$

The differential, $d\tau_{jl}^{abs}$, is the incremental departure from the base optical depth, τ_l, existing prior to the enhancement of absorber j. We will use the finite difference form of (8) because a differential change in τ will result in a negligible change in I

$$\delta_{jl} = \frac{\Delta \ln I}{\Delta \tau_{jl}^{abs}} = \frac{-\ln \frac{I}{I'}}{\sigma_j^{abs} \Delta N_{jl}}. \tag{9}$$

This formalism can be applied to the case where one or more of the layers is initially optically thick. Observations obtained at a specific solar zenith angle (say 90°) are commonly used to obtain total slant column abundance of the absorbing species. The air mass values can also be used to analyze observations taken at several solar zenith angles during twilight. This leads to the inverse problem of retrieving the absorber profile from a measured time series of slant columns [*McKenzie et al.*, 1991].

Three radiative transfer models will be used to compute zenith intensities at the ground before and after introducing optically thin ($\tau_{jl}^{abs} < 0.01$) absorbing layers from which the air mass δ_{jl} is determined using (9). A fourth model will also be considered that is based on a different formulation of the air mass.

3. Computation of Air Mass

Air mass may be calculated in two different ways. The first method [*Perliski*, 1992] determines the air mass by computing zenith intensities at the ground level and using (9). The second method is based on a weighting scheme [*Dahlback et al.*, 1994] which is useful if multiple scattering is unimportant. It is justified as follows.

Weighting Method

The atmosphere is divided into L adjacent layers shown in Figure 1. For simplicity we consider single scattering only. We assume that all single-scattering events along the vertical line within layer l take place at the midpoint of layer l, i.e., at an effective scattering height. The intensity of radiation in the nadir direction that has been scattered once within layer l is denoted by I_l. Before entering the detector, these photons follow a vertical path and are attenuated by a factor $e^{-\tau_l}$, where $-\tau_l$ is the vertical optical depth (scattering plus absorption) from the center of layer l to the detector at the ground.

The total intensity of singly scattered photons from the zenith direction at the ground, i.e., the contributions from all layers, is

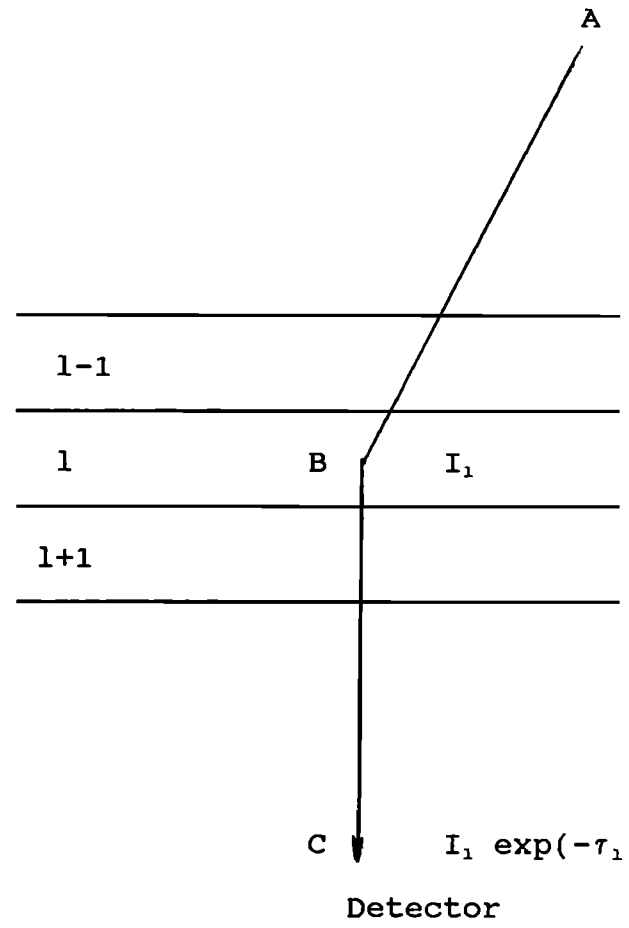

Figure 1. The geometry of the weighting method. We consider single scattering only. Direct sunlight is scattered at all levels within layer l into the nadir direction. We assume that all the scatterers within layer l are located at the center of the layer, at point B. The intensity of the radiation from the zenith direction at point B due to all the radiation scattered once within layer l is denoted by I_l. This radiation is attenuated by $\exp(-\tau_l)$ where τ_l is the total vertical optical depth (absorption plus scattering) between the center of the layer, B, and the ground, C. τ_l^{abs} is the sum of the slant optical path due to the absorber, between A and B, and the vertical optical depth due to the absorber, between B and C.

$$I_{total} = \sum_{l=1}^{L} I_l e^{-\tau_l}. \tag{10}$$

The probability that the singly scattered radiation received by the detector arises from scattering within layer l can be described by the probability density function

$$P_l = \frac{I_l e^{-\tau_l}}{\sum_{l=1}^{L} I_l e^{-\tau_l}}. \tag{11}$$

The slant optical thickness (A to B in Figure 1) due to the absorber before radiation is scattered, plus the vertical optical depth (B to C in Figure 1) due to the absorber once it is scattered, is denoted by τ_l^{abs}. The effective absorber optical path, τ_{eff}^{abs} (slant plus vertical) is defined by weighting the var-

ious absorber optical depths τ_l^{abs}, with the probability density function, P_l

$$\tau_{eff}^{abs} = \sum_{l=1} P_l \tau_l^{abs}. \quad (12)$$

The air mass is obtained by taking the ratio between the effective absorber optical path, τ_{eff}^{abs}, and the total absorber (vertical) optical depth, τ^{abs}. To account for multiple scattering, the computation of I_l appearing in the probability function, P_l, includes all orders of scattering. Photons cannot be scattered back into the beam between the center of l and the ground.

Radiative Transfer Models

To calculate the zenith intensities needed in (9) and (12), three different radiative transfer models accounting for spherical geometry were used. Below, we briefly outline each of the models.

Discrete ordinate method. The discrete ordinate solution to the radiative transfer equation described by *Stamnes et al.* [1988] has been modified to include the curvature of the atmosphere [*Dahlback and Stamnes*, 1991]. This is done in an approximate manner using a geometrical correction to treat the direct beam so that (5) becomes

$$u \frac{\partial I(-r, u)}{\partial r} + \frac{1 - u^2}{r} \frac{\partial I}{\partial u} = -k(r)[I - S] \quad (13)$$

where

$$S(r, u) = \frac{a(r)}{2} \int_{-1}^{1} p(r, u, u') I(r, u')\, du' + \frac{a(r)}{4\pi} p(r, u, u') F^s \exp[-\tau Ch(r, \mu_0)]. \quad (14)$$

Here

- I azimuthally averaged scattered intensity;
- r radial distance from the center of the Earth;
- u cosine of the polar angle;
- k extinction coefficient;
- S source function;
- a single-scattering albedo;
- p scattering phase function;
- μ_0 cosine of the solar zenith angle;
- F^s flux at the top of the atmosphere (normal to the beam);
- τ optical depth;
- Ch geometrical correction due to a curved atmosphere, generally referred to as the Chapman function [*Dahlback and Stamnes*, 1991].

As noted previously (after equation (3)) in plane geometry, $Ch = 1/\mu_0$, and the second term of the left-hand side of (13) proportional to $\partial I/\partial u$ disappears. In the pseudospherical approximation the second term on the left-hand side of (13) is ignored. The resulting equation is similar to the plane-parallel equation, except that the direct beam attenuation includes the effect of spherical geometry. For our purposes this approximation yields accurate results as discussed in some detail by *Dahlback and Stamnes* [1991]. The atmosphere is divided into a suitable number of layers to resolve the optical properties adequately. An exponential-linear in optical depth approximation is used to compute the direct beam source within each layer [*Kylling and Stamnes*, 1992]. With these modifications, zenith intensities that include all orders of scattering can be computed accurately under twilight conditions.

Monte Carlo method. The backward Monte Carlo method works as follows: The propagation of light through a spherical shell, scattering, and optically thin absorbing atmosphere is simulated by first allowing light to emerge in a given direction from a hypothetical detector. The directions and optical distances between each subsequent scattering event are then simulated as a random walk process, with the probability of a scattering event occurring at a particular location taken to be proportional to the local scattering coefficient. The direction the scattered light takes is selected randomly by consideration of either the Rayleigh or the Mie scattering phase function, depending on whether molecular or aerosol scattering occurred. The scattering coefficient is determined by multiplying the cross section with the concentration of the scattering species.

Absorption is computed along each scattering path and along the direct-solar-beam path. The combination of the direct beam and the particular path of a scattering species to the detector constitutes an "intensity history." In general, on the order of one thousand intensity histories are computed and averaged for each solar zenith angle considered, resulting in a zenith intensity for each "final scattering" altitude. The backward Monte Carlo technique used in this study is described in more detail by *Perliski* [1992] and is conceptually similar to that described by *Collins et al.* [1972], *Adams and Kattawar* [1978], *Kattawar and Adams* [1978], and *Lenoble and Chen* [1992].

Integral equation method. The integral equation method radiative transfer model solves the integral equation for transfer of radiation (equation (4b)) and thus yields the total source function or total radiance integrated over 4π steradians [*Anderson and Lloyd*, 1990]. To calculate zenith intensities, one first computes the direct and the multiply scattered portions of the total (angularly integrated) intensities as a function of altitude, i.e., the source functions. These source functions (equation (4b)) are then integrated along the zenith direction, accounting for the optical depth between the source at a given altitude and the ground (equation (5)). When phase functions are used, they are only applied to the singly scattered source functions (first term of equation (4b)); it is assumed that the multiply scattered radiation is isotropic. This model includes spherical geometry at large solar zenith angles ($\geq 60°$) for the calculation of the incident radiation.

4. Results of Air Mass Computations

Four methods were used to calculate air mass. They are DISORT I, discrete ordinate method using (9) by computing ratios of zenith intensities; DISORT II, discrete ordinate method using the weighting scheme described by (10)–(12); Monte Carlo, Monte Carlo statistical method using (9); integral equation method using (9).

Air mass was computed for two absorber heights at two wavelengths. In the first case, a 5.0-km thick NO_2 layer of total column abundance 3.0×10^{15} cm^2 was placed between 20 and 25 km. In the second case, the same layer was placed between 0 and 5 km. Air mass was computed at solar zenith angles from 70° to 95° in 1° increments at two wavelengths, $\lambda = 450$ and 650 nm. U.S. Standard Atmosphere profiles for ozone, temperature and pressure were used with 75 layers, each 1 km thick;

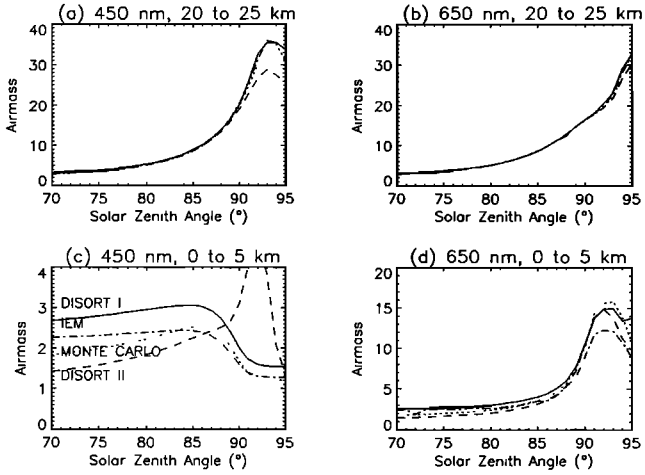

Figure 2. Air mass computed using four different methods: DISORT I (solid), Monte Carlo (dotted), DISORT II (dashed), and integral equation method (IEM) (dashed-dotted). Computations were performed with the absorber between 20 and 25 km at (a) 450 nm and (b) 650 nm. The absorber was between 0 and 5 km at (c) 450 nm and (d) 650 nm.

the surface albedo was set to 0.3. To simplify the comparison, all the computations were performed using isotropic scattering. It was found, using DISORT I, that the air mass values computed for Rayleigh and isotropic scattering were within 5% of each other for these four cases: (1) tropospheric absorber, solar zenith angle of 60°; (2) stratospheric absorber, solar zenith angle of 60°; (3) tropospheric absorber, solar zenith angle of 90°; (4) stratospheric absorber, solar zenith angle of 90°.

Figure 2 shows air mass versus solar zenith angle for $\lambda = 450$ nm and 650 nm for the four methods with the absorber between 0 and 5 km and 20 and 25 km. Figure 2a shows the case for a stratospheric absorber at 450 nm. We will focus on air mass values computed at 90° because this is a solar zenith angle typically used for conversion of measured slant to vertical columns. Arbitrarily choosing DISORT I as a basis of comparison, we find agreement between the different methods is within 6.0% at a solar zenith angle of 90°. Figure 2b shows results for $\lambda = 650$ nm with the absorber between 20 and 25 km. Again the agreement is within 6% at 90°. Thus when the bulk of NO_2 is in the stratosphere, as is the case in the absence of tropospheric NO_2 pollution, the four methods yield satisfactory agreement at 90°. At larger solar zenith angles the difference is larger, becoming as large as 27% between DISORT I and DISORT II at 95° at 450 nm.

The agreement at 90° solar zenith angle is not so good when the absorber is located in the troposphere. At 450 nm the difference between Monte Carlo and DISORT I at 90° is 21% (Figure 2c), and at 650 nm the difference between DISORT I and DISORT II is 4% (Figure 2d). Even greater differences between the two air mass formulations (DISORT I and DISORT II) occur at larger solar zenith angles, amounting to more than 50% at 92°.

To investigate the reasons for the poor agreement for a tropospheric absorber, the DISORT I and Monte Carlo zenith intensities at 90° were compared as shown in Table 1 (tropospheric absorber) and Table 2 (stratospheric absorber). The best agreement (within 0.7%) is at 450 nm for a tropospheric absorber, and the worst agreement (about 4.5%) is at 650 nm for a tropospheric absorber. Results from the other two models agreed to within 2% of DISORT I and have been omitted. Note the very close agreement in the ratio of zenith intensities with and without absorber (I'/I). In spite of the small differences in these ratios, taking the natural log of the intensity ratio (equation (9)) results in a larger difference in air mass. The reason is that for small x, $\ln(1 - x)$ is close to $-x$. For instance, at 450 nm with a tropospheric absorber (the worst agreement among the four cases) the DISORT I and Monte Carlo intensity ratios differ by only 0.05%, yet their log ratios (and hence the air mass values) differ by 17%.

The weighting method (used in DISORT II) gives good agreement with the other three models for a stratospheric absorber where multiple scattering is minimal but poorer agreement for a tropospheric absorber where multiple scattering is significant. As mentioned, the weighting method does not allow photons to be scattered back into the beam between the last scattering event and the ground, which is likely the source of this method's disagreement with the other three models.

5. Conclusions

Air mass values relevant for measurement of NO_2 have been computed using four different methodologies. The agreement among the four methods is within 6% at 90° solar zenith angle at 450 and 650 nm when the absorber is in the stratosphere. Thus the conversion of 90° solar zenith angle slant column abundances to vertical column abundances using these air mass values will agree to within 6% for a stratospheric absorber. Larger differences in air mass occur when the absorber is in the troposphere where multiple scattering becomes significant. Because the absorption for tropospheric absorbers at large zenith angles is small, the ratio of intensities with and without absorbers is very close to 1. Therefore slight differences in zenith intensities lead to significant differences in air mass values. Practically speaking, these differences in tropospheric air mass values are not critical to the community of stratospheric spectroscopists interested in measuring NO_2, BrO, or OClO column abundances because there is normally

Table 1. Comparison of 90° Zenith Intensities With and Without Tropospheric NO_2

λ nm	DISORT I × 10^3	Ratio DISORT I/I'	Monte Carlo × 10^3	Ratio MC I/I'	Percent Difference (MC-DIS)/DIS	Percent Difference Air Mass
450 NO_2	2.379	0.9971	2.365	0.9976	−0.59	17.4
Without	2.386	···	2.370	···	−0.67	···
650 NO_2	1.318	0.9992	1.263	0.9994	−4.17	3.6
Without	1.319	···	1.263	···	−4.25	···

MC, Monte Carlo; DIS, DISORT.

Table 2. Comparison of 90° Zenith Intensities With and Without Stratospheric NO_2

λ nm	DISORT $I \times 10^3$	Ratio DISORT I/I'	Monte Carlo $\times 10^3$	Ratio MC I/I'	Percent Difference (MC-DIS)/DIS	Percent Difference Air Mass
450 NO_2	2.315	0.9702	2.300	0.9704	−0.65	2.0
Without	2.386	...	2.370	...	−0.65	...
650 NO_2	1.318	0.9992	1.268	0.9991	−3.79	0.6
Without	1.319	...	1.270	...	−3.71	...

very little of these gases in the troposphere. For a solar zenith angle of 90° the air mass for a stratospheric absorber is typically 10 times that of a tropospheric absorber making this method less sensitive to tropospheric NO_2 and to errors in tropospheric air mass. However, if significant tropospheric pollution were present, differences would ensue between air mass values computed by these methods. In practice, one must look at the twilight time series of slant column measurements to ensure that the measurements are unpolluted. Only when the tropospheric component of the absorber is large and changes with time in an unpredictable manner does the twilight method fail. In such cases, easily discerned by an inspection of the twilight time series, it is difficult to separate the tropospheric and stratospheric components. Even in the presence of a fairly large but unchanging tropospheric component, the twilight method can be corrected for tropospheric pollution.

Only the Monte Carlo method treats the scattered radiation in spherical geometry and is therefore the most accurate for tropospheric air masses where multiple scattering is significant. The discrete ordinate and integral equation models use a conceptual approximation by treating the scattered radiation in plane parallel geometry. Air mass values computed using the weighting method (used in DISORT II) show the largest disagreements with the other three methods for a tropospheric absorber. The reason is probably that this formulation fails to treat multiple scattering completely. However, for absorbers in the stratosphere, major saving of computing time without any loss of accuracy is obtained using the discrete ordinate or integral equation method. A DEC-5000 work station running ULTRIX for the discrete ordinate method took about 60 s for 26 solar zenith angles at one particular wavelength. For the integral equation method (IEM) running on a silicon graphics challenge work station, for 26 solar zenith angles, the computing time was about 1600 s. Although the IEM method in these computations did not include refraction, still the refraction routines were called. If these routines were removed from the model, these computations could be performed in less than 60 s. This compares with execution times of about 2500 s for these same computations using the Monte Carlo technique running on a Cray YMP.

Acknowledgments. Thanks to the helpful comments of two anonymous reviewers and to the suggestions of H. K. Roscoe.

References

Adams, C. N., and G. W. Kattawar, Radiative transfer in spherical shell atmospheres, I, Rayleigh scattering, *Icarus*, *35*, 139–151, 1978.

Anderson, D. E., Jr., and S. A. Lloyd, Polar twilight UV-visible radiation field: Perturbations due to multiple scattering, ozone depletion, stratospheric clouds, and surface albedo, *J. Geophys. Res.*, *95*, 7429–7434, 1990.

Brewer, A. W., C. T. McElroy, and J. B. Kerr, Nitrogen dioxide concentration in the atmosphere, *Nature*, *264*, 129–133, 1973.

Collins, D. G., W. G. Blattner, M. B. Wells, and H. G. Horak, Backwards Monte Carlo calculations of the polarization characteristics of the radiation emerging from a spherical shell atmosphere, *Appl. Opt.*, *11*, 2684–2696, 1972.

Dahlback, A., and K. Stamnes, A new spherical model for computing the radiation field available for photolysis and heating at twilight, *Planet. Space Sci.*, *39*, 671–683, 1991.

Dahlback, A., P. Rairoux, B. Stein, M. Del Gusta, E. Kyro, and L. Stefanutti, Effects of stratospheric aerosols from the Mt. Pinatubo eruption in ozone measurements at Sodankylä, Finland, *Geophys. Res. Lett.*, *21*, 1391–1402, 1994.

Harrison, A. W., Midsummer stratospheric NO_2 at 45°S, *Can. J. Phys.*, *57*, 1110–1117, 1979.

Johnston, P. V., R. L. McKenzie, J. G. Keys, and W. A. Matthews, Observations of depleted stratospheric NO_2 following the Pinatubo volcanic eruption, *Geophys. Res. Lett.*, *19*, 211–213, 1992.

Kattawar, G. W., and C. N. Adams, Radiative transfer in spherical shell atmospheres, II, asymmetric phase functions, *Icarus*, *35*, 436–453, 1978.

Kylling, A., and K. Stamnes, Efficient yet accurate solution of the linear transport equation in the presence of internal sources: The exponential-linear-in-depth approximation, *J. Comput. Phys.*, *102*(2), 265–276, 1992.

Lenoble, J., and H. B. Chen, Monte Carlo study of the effects of stratospheric aerosols and clouds on zenith sky absorption measurements, paper presented at Symposium on International Radiation, Int. Assoc. of Meteorol. and Atmos. Phys. (IUGG), Tallin, Aug. 1992.

McKenzie, R. L., and P. V. Johnston, Seasonal variations in stratospheric NO_2 at 45°S, *Geophys. Res. Lett.*, *9*, 1255–1258, 1982.

McKenzie, R. L., P. V. Johnston, C. T. McElroy, J. B. Kerr, and S. Solomon, Altitude distributions of stratospheric constituents from ground-based measurements at twilight, *J. Geophys. Res.*, *96*, 15,499–15,511, 1991.

Mount, G. W., R. W. Sanders, A. L. Schmelteklopf, and S. Solomon, Visible spectroscopy at McMurdo Station, Antarctica, 1, Overview and daily variations of NO_2 and O_3: Austral spring, 1986, *J. Geophys. Res.*, *92*, 8320–8328, 1987.

Noxon, J. F., Nitrogen dioxide in the stratosphere and troposphere measured by ground based absorption spectroscopy, *Science*, *189*, 547–549, 1975.

Perliski, L. M., The role of multiple scattering in twilight zenith sky observations of atmospheric absorbers: Diurnal photochemistry and air mass factors, Ph.D. thesis, 178 pp., Univ. of Colo., Boulder, 1992.

Perliski, L. M., and S. Solomon, Radiative influences of Pinatubo volcanic aerosols on twilight observations of NO_2 column abundances, *Geophys. Res. Lett.*, *19*, 1923–1926, 1992.

Perliski, L. M., and S. Solomon, On the evaluation of air mass factors for atmospheric near-ultraviolet and visible absorption, *J. Geophys. Res.*, *98*, 10,363–10,374, 1993.

Pommereau, J. P., and F. Goutail, Stratospheric O_3 and NO_2 observations in the southern polar circle in summer and fall 1988, *Geophys. Res. Lett.*, *15*, 895–897, 1988.

Sarkissian, A., H. K. Roscoe, D. Fish, M. Van Roozendael, M. Gil, H. B. Chen, P. Wu, J.-P. Pommereau, and J. Lenoble, Ozone and NO_2 air-mass factors for zenith-sky spectrometers: Intercomparison of calculations with different radiative transfer models, *Geophys. Res. Lett.*, *22*, 1113–1116, 1995.

Schiller, C., A. Wahner, U. Platt, H.-P. Dorn, J. Callis, and D. Ehhalt, Near UV atmospheric absorption measurements of column abun-

dances during Airborne Arctic Stratospheric Expedition, January–February, 1989, 2, OClO observations, *Geophys. Res. Lett.*, *17*, 510–504, 1990.

Solomon, S., R. W. Sanders, M. A. Carroll, and A. L. Schmeltekopf, Visible and near-ultraviolet spectroscopy at McMurdo Station, Antarctica, 5, Diurnal variations of OClO and BrO, *J. Geophys. Res.*, *94*, 11,393–11,398, 1989.

Stamnes, K., S.-C. Tsay, W. Wiscombe, and K. Jayaweera, Numerically stable algorithm for discrete-ordinate-method radiative transfer in multiple scattering and emitting layered media, *Appl. Opt.*, *27*, 2502–2509, 1988.

D. Anderson and R. DeMajistre, Applied Physics Laboratory, Johns Hopkins University, Laurel, MD 20723-6099.

A. Dahlback, Norwegian Institute for Air Research, Kjeller N 2007, Norway.

K. Hammond, Department of Physics, University of Minnesota, Minneapolis, MN 55418.

A. Kylling and K. Stamnes, Geophysical Institute, University of Alaska, Fairbanks, AL 99775-0800.

L. Perliski, Geophysical Fluids Dynamics Laboratory, Princeton, NJ 08542.

J. Slusser (corresponding author), Centre for Atmospheric Science, Department of Chemistry, Cambridge University, Cambridge, U.K. CB2 1EW.

(Received October 18, 1994; revised October 12, 1995;
accepted November 17, 1995.)